DOI: 10.15669/pnst.7.250

Progress in Nuclear Science and Technology
Volume 7 (2025) pp. 250-256

ARTICLE

Novel seawater desalination technology with liquid metal fluid

Toranosuke Horikawa [a] and Masatoshi Kondo [b *]

[a] *Institute of Science Tokyo, School of Engineering, Department of Mechanical Engineering, Graduate Major in Nuclear Engineering, Ookayama, Meguro-ku, Tokyo 152-8550, Japan;* [b] *Institute of Science Tokyo, Institute of Integrated Research, Laboratory for Zero-Carbon Energy, Ookayama, Meguro-ku, Tokyo 152-8550, Japan*

Seawater desalination is one of the promising solutions to address serious water shortage. However, conventional methodologies of seawater desalination require the large consumption of electricity and the brine discharge which can cause an environmental load. Seawater mining provides a sustainable development perspective of human society. The present study proposes the novel desalination process without the brine discharge, in which desalinated water is produced by a repetitive distillation process and liquid metal tin recovers the mineral elements contained in seawater. Desalinated water is produced by the direct contact between seawater and liquid metal tin heated by solar thermal energy. The mass transfer of mineral elements between seawater and liquid metal tin was clarified by means of direct contact tests. The purity of the distilled water was sufficiently high, though small contamination with mineral elements was caused by the transfer of artificial seawater particles produced in the distillation process. The dissolution and mass transfer of mineral elements such as Na, Mg and Cl in liquid tin were metallurgically analyzed. The collective results of the present study motivate freshwater production and valuable elements recovery, which promote a sustainable society through the liquid metal-based seawater desalination technology.

Keywords: seawater desalination; seawater mining; distillation; liquid metal

1. Introduction

Freshwater is a core resource for human society and economic stability. However, freshwater scarcity is a serious problem. About 4.0 billion people suffered from severe water scarcity at least one month in one year [1]. Seawater desalination is one of the promising methods to satisfy the huge demand of freshwater [2]. However, conventional technologies such as reverse osmosis (RO) and multi-stage flash (MSF) are prospective for adverse environmental impacts due to high energy consumption and brine discharge [3,4]. The RO requires large electricity consumption for the freshwater production even when the scale of desalination plant is small (e.g., 17 kWh/m^3) [5], though the energy consumption rate can be improved according to the increase of plant scale (e.g., 2 kWh/m^3) [6]. The global brine production is 141.5 million m^3/day, which is 1.5 times larger than the desalinated water [7]. The brine discharge to the marine environment can induce compositional and physiological changes in marine species due to a change in the water salinity [8]. Therefore, the development of sustainable and environment-friendly seawater desalination technology is urgently required in the critical era of severe water scarcity [9]. Sustainable sourcing of valuable elements is necessary for a growing demand according to a growing global population [10]. The ocean can provide abundant valuable resources as seawater mining though their concentrations in seawater are very low [11].

The concept of liquid metal direct contact boiling heat and mass transfer has been studied for the application in Pb-Bi cooled fast reactors [12]. The application of direct contact heat and mass transfer between seawater and liquid lead alloys was conceptually studied for the production of pure water in some previous studies [13-15], though it has been rarely demonstrated by the experiment. The present study proposes novel seawater desalination technology based on the circulation system of liquid metal tin (Sn: melting point 505 K) with solar thermal energy as shown in **Figure 1**. Liquid metal Sn reveals low toxicity and excellent thermal properties such as high heat conductivity and low vapor pressure [16]. Liquid metal Sn has strong chemical affinity with metal elements [17]. Pure water is produced in the distillation process by the direct contact between seawater and liquid metal Sn. The mineral elements (e.g., Na, Mg, Li, K, Rb, Cl, etc.) dissolved in seawater are recovered by liquid metal Sn. Therefore, brine and scale are not discharged, and the environmental load of the current desalination process is

*Corresponding author.
E-mail: kondou.m.fdb5@m.isct.ac.jp (Masatoshi Kondo)

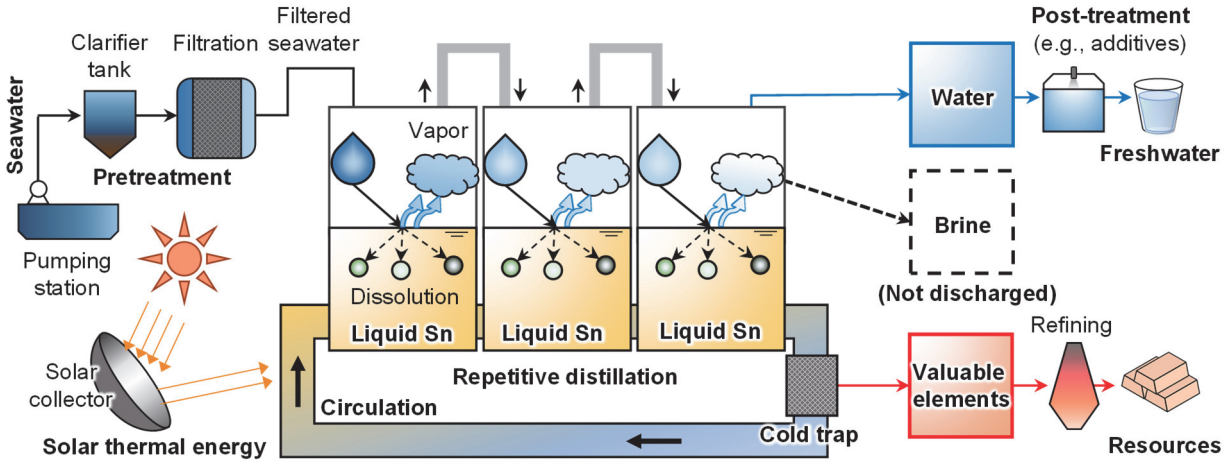

Figure 1. Schematic diagram of seawater desalination and resource recovery process with liquid Sn.

very small. This desalination process can provide a significant contribution to solve the problem of water and resource scarcity in the world.

The seawater desalination is performed in the high temperature region of the liquid Sn circulation system. Seawater is directly splayed to the free surface of liquid Sn after the removal of sludge, suspended organics, fine particles, bacteria, oil and so on in the pretreatment procedure of seawater [18]. The desalinated water is treated with additives for disinfection and pH control in the post-treatment procedure. The mineral elements dissolved in liquid Sn are continuously recovered in the cold trap, in which the elements are oversaturated and precipitated in a lower temperature condition [19]. The non-metal elements (e.g., Cl, H and O) are going to be removed from liquid Sn by thermal desorption method [20]. The energy conversion efficiency between solar thermal energy to heat energy is very high as approximately 0.56 [21]. If the high temperature condition of liquid Sn is kept by the direct use of solar thermal energy, the electricity consumption of this desalination system can be greatly reduced.

The purpose of the present study is to clarify the mass transfer between liquid Sn and seawater. The direct contact tests between droplets of artificial seawater and liquid Sn were performed. The purity of water produced by the distillation process was investigated. The metallurgical analysis on the Sn media which was exposed to artificial seawater was performed to clarify the mass transfer of mineral elements in liquid Sn. The collective results of this study motivate freshwater production and valuable elements recovery, which promote a sustainable society through the novel seawater desalination technology.

2. Experimental conditions

The direct contact tests of artificial seawater and liquid Sn were performed at the conditions presented in **Table 1**. The chemical compositions of artificial seawater and the purity condition of Sn are presented in **Table 2** and **Table 3**, respectively. The artificial sea salt (provided from Kaisuimaren Co.) of 3.5 g was dissolved in distilled water of 1 L to make artificial seawater. The tests with liquid Sn at 523K, 573K and 623K were performed under air atmosphere at atmospheric pressure. The droplets of artificial seawater

Table 1. Experimental conditions.

Specimens	Temperature [K]	State	Seawater quantity [mL]	Duration [min]	Dripping ratio [mL/min]
Sn	473	Solid	5	50	0.1
Sn	523	Liquid	5	50	0.1
Sn	573	Liquid	5	50	0.1
Sn	623	Liquid	5	50	0.1
316L	473	Solid	5	50	0.1
316L	573	Solid	5	50	0.1

Table 2. Chemical composition of artificial seawater used in current work (unit: mg/L).

Cl	Na	Mg	S	Ca	K	Br	Sr	B	Mo	Mn
19,040	10,500	1,350	2,400	400	380	4.9	8.00	8.2	0.06	0.002

Table 3. Purity condition of Sn used in current work (unit: wt.%).

Cu	Pb	Sb	Fe	In	Zn	Sn
0.0015	0.0006	0.0004	0.0004	0.0004	0.0001	Bal.

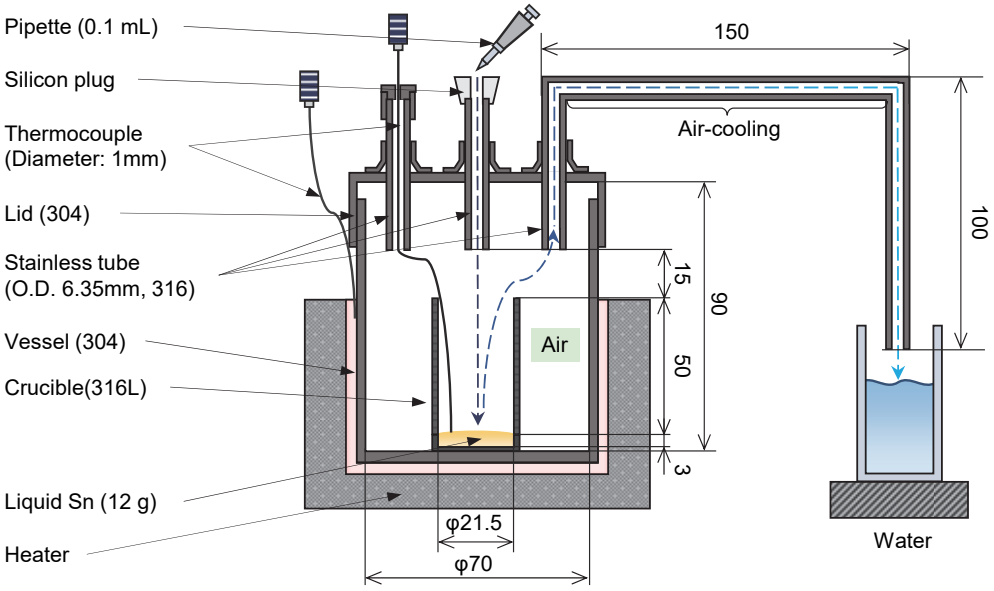

Figure 2. Schematic diagram of apparatus for seawater direct contact distillation test.

were continuously dripped onto the surface of liquid Sn, and the distilled water of 3 mL was recovered in the tests. The diameter of droplet was approximately 5 mm. The temperature of seawater was room temperature. The direct contact tests with plates of solid Sn and 316L austenitic steel (Fe-18Cr-12Ni-2Mo) were also performed as reference.

Figure 2 shows the schematic diagram of the apparatus used for the seawater direct contact distillation test. Liquid Sn of approximately 12 g was installed in the crucible which was made of 316L. The height of the stainless crucible was 50 mm. The 316L plate specimen was installed in the crucible for the reference experiment. The outer diameter and thickness of 316L plate specimen were 21.5 mm and 3 mm, respectively. The temperature of liquid Sn was controlled by the heater installed on the outside of the vessel and the thermocouple inserted into the melt.

The impurity concentration of the water distilled was measured with an inductively coupled plasma optical emission spectrometer (ICP-OES, Agilent Technology; 5100 VDV ICP-OES). The Cl^- concentration in the water distilled was measured by a silver nitrate visual colorimetric method. The concentration of HClO in the water distilled was measured by a potassium iodide visual colorimetric method. The surface of Sn and 316L used in the direct contact tests was observed and analyzed with a scanning electron microscope (SEM, Keyence; VE9800) with an energy-dispersive X-ray spectrometer (EDX, AMETEK; Genesis XM2). The chemical compounds formed on the surface of Sn and 316L were identified by a thin film X-ray diffraction measurement (XRD, Maven Panalytical; X' Pert-Pro-MRD). The surface cross section of Sn and 316L tested was observed and analyzed with the SEM/EDX after the sequential polish with SiC papers of #500, #1200, #2000 and #4000 and ethanol as a lubricant.

3. Experimental results

3.1. Purity of water distilled in direct contact tests with liquid Sn

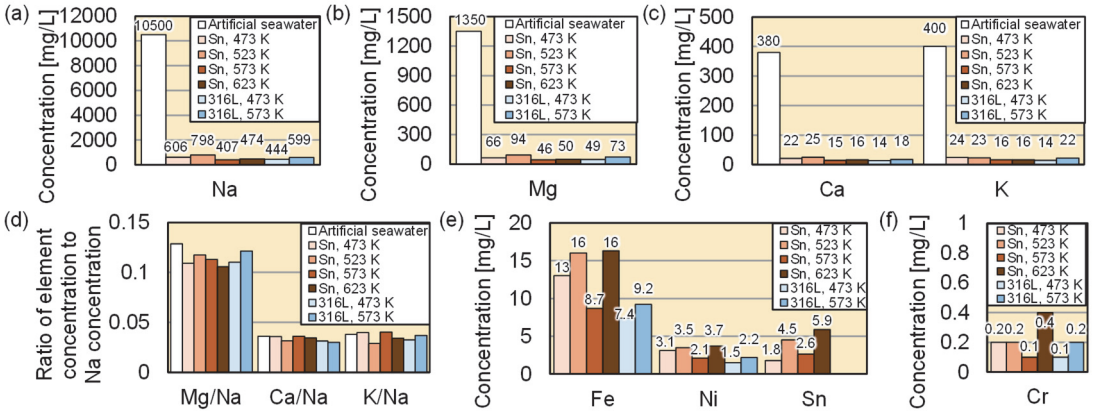

Figure 3. Concentrations of mineral and metal elements in water distilled by direct contact tests: (a) Concentration of Na, (b) Concentration of Mg, (c) Concentrations of Ca and K, (d) Ratio between concentrations of Mg, Ca and K elements to that of Na, (e) Concentrations of Fe, Ni and Sn and (f) Concentration of Cr.

Figures 3 (a), (b) and **(c)** show the concentrations of mineral elements in water distilled in the direct contact distillation tests. The concentrations of Na, Mg, Ca and K in the water distilled in all the tests were smaller than 1,000 mg/L, which satisfied the drinking water quality standard set by World Health Organization (WHO) [22]. However, Na, Mg, Ca and K were slightly detected in the distilled water. The concentration of Na in the distilled water was higher than that in tap water in Japan (e.g., 10.7 mg/L) [23]. The ratios between the concentrations of Mg, Ca and K elements (i.e., C_{Mg}, C_{Ca} and C_K) to that of Na (i.e., C_{Na}) were shown in **Figure 3 (d)**. The ratios of C_{Mg}/C_{Na}, C_{Ca}/C_{Na} and C_K/C_{Na} in the distilled water were the same with those in the artificial seawater used in the present study. The Cl^- concentration in the distilled water was almost the same with that of Na. HClO was not detected in the distilled water. Therefore, these results indicated that the contamination of distilled water with mineral elements could be caused by the particle transport of artificial seawater as described in the chapter of discussions. The removal ratio of elements contained in seawater in the single distillation process was estimated as approximately 95-97 % in the current work. The purity of distilled water could be improved by a repetitive procedure. **Figures 3 (e)** and **(f)** show the concentrations of Sn and elements in the water, which are contained in the materials of vessel and crucible. The concentrations of Fe, Cr and Ni didn't satisfy the WHO standard. The Sn contamination of distilled water was possibly due to the transfer of Sn particles along vapor flow.

3.2. Mass transfer of mineral elements between liquid Sn and artificial seawater

Figures 4 (a) and **(b)** show the SEM surface images of the 316L plates used in the direct contact tests at 473 K and 573 K, respectively. **Figures 5 (a)** and **(b)** show the results of XRD analysis on the surfaces of the 316L plates used in the direct contact tests at 473 K and 573 K, respectively. These results indicated that NaCl crystals grew on the 316L surface, though the size of salt crystals deposited in the test at 573 K was larger than that at 473 K. **Figure 4 (g)** shows the result of EDX element mapping analysis on the 316L plate tested at 573 K. Mg was detected in the region where Na and Cl were not detected. **Figure 4 (c)** and **Figure 5 (c)** show the results of SEM observation and XRD analysis on the surface of Sn tested in a solid-state condition at 473 K, respectively. The cubic crystals of NaCl were detected on the surface as the same as those detected on the 316L surface.

Figures 4 (d) and **(e)** show the SEM surface images of the Sn tested in a liquid-state condition at 523 K and 573 K, respectively. **Figures 5 (d)** and **(e)** show the results of XRD analysis on the surfaces of Sn tested in a liquid-state condition at 523 K and 573 K, respectively. The crystals

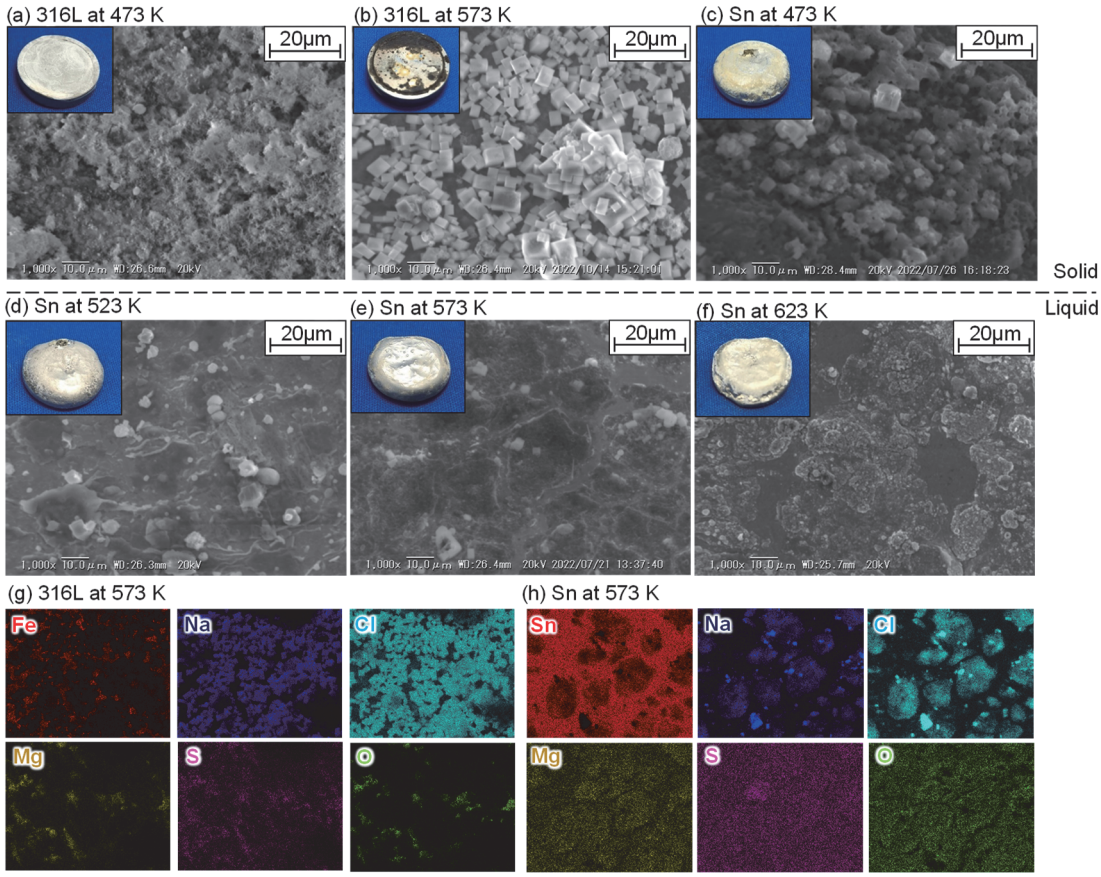

Figure 4. SEM surface images: (a) 316L tested at 473 K, (b) 316L tested at 573 K, (c) Sn tested at 473 K, (d) Sn tested at 523 K, (e) Sn tested at 573 K, (f) Sn tested at 623 K, (g) EDX mapping analysis on 316L tested at 573 K and (h) EDX mapping analysis on Sn tested at 573 K.

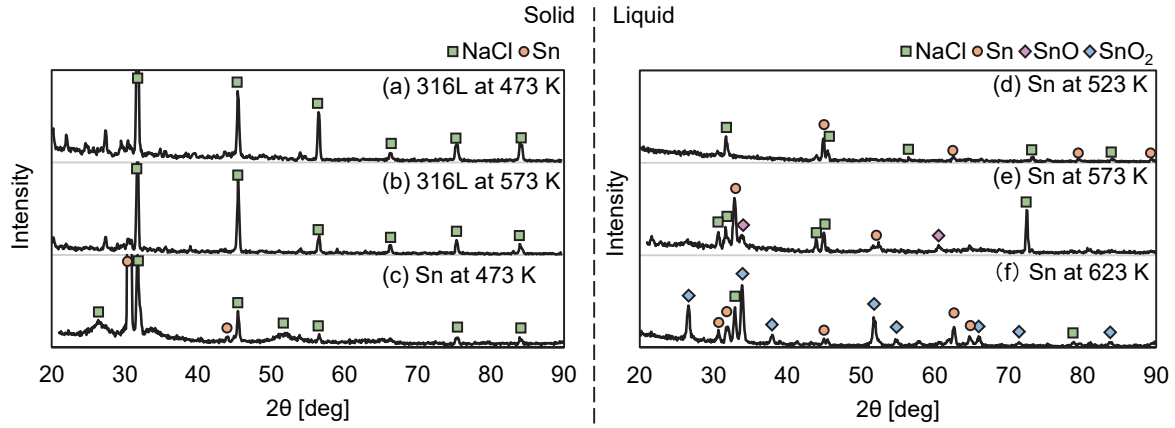

Figure 5. XRD analysis on surfaces of 316L and Sn used in direct contact tests: (a) 316L tested at 473 K, (b) 316L tested at 573 K, (c) Sn tested at 473 K, (d) Sn tested at 523 K, (e) Sn tested at 573 K and (f) Sn tested at 623 K.

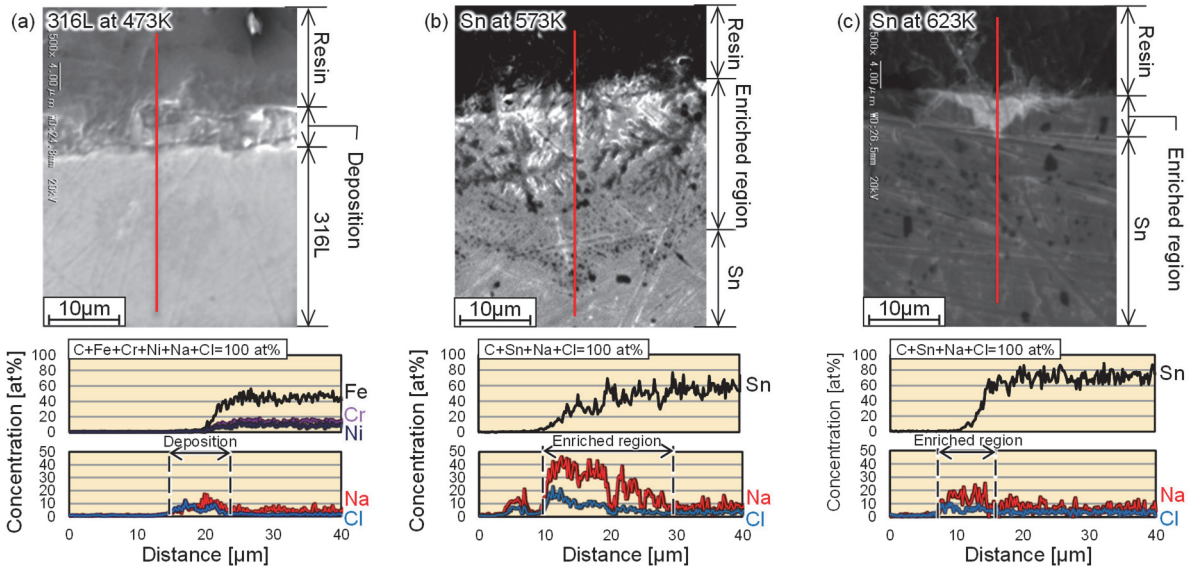

Figure 6. SEM/EDX cross-sectional analysis on surfaces of 316L and Sn used in direct contact tests: (a) 316L tested at 473 K, (b) Sn tested at 573 K and (c) Sn tested at 623 K.

of NaCl were rarely detected on their surfaces, though they were clearly detected on the 316L plate and solid Sn.

Figures 4 (h) shows the result of EDX element mapping analysis on the Sn tested at 573 K. Mg was detected in the region where Na and Cl were detected. **Figure 4 (f)** shows the SEM surface image of the Sn tested in a liquid-state condition at 623 K. The formation of SnO_2 was recognized as shown in **Figure 5 (f)**. Na and Mg were dissolved in liquid Sn. The oxides of Na and Mg (i.e., Na_2O and MgO) are thermodynamically stable more than the oxide of Sn, though the current results could not provide any evidence supporting the dissolution of Na and Mg into liquid Sn in an atomic state. Therefore, the oxidation of Sn may be inhibited due to the sacrificial oxidation of Na dissolved in liquid Sn during the longer-term operation. **Figure 6 (a)** shows the result of SEM/EDX cross-sectional analysis on the surface of 316L plate used in the test at 473 K. The deposition of salt on the surface was recognized. **Figure 6 (b)** shows the surface cross section of Sn tested in a liquid-sate condition at 573 K. Na and Cl were detected near the surface of Sn matrix. The dissolution of Na and Cl into the Sn matrix from artificial seawater was indicated by the profiles of their concentrations. The depth of the Na and Cl enriched region was approximately 20 μm. The atomic concentration of Na could be the same with that of Cl when NaCl dissolved and deposited in the region. However, the atomic concentration of Na was twice higher than that of Cl. These results indicated that Na and Cl atoms separately dissolved and transferred in liquid Sn. Oxygen was detected in the region, and the atomic concentration of O was almost the same with that of Na. Therefore, the detection of oxygen was possibly due to the formation of NaOH on the preparation procedure of the surface cross section. **Figure 6 (c)** shows the surface cross section of Sn tested in a liquid-state condition at 623 K. The Na and Cl were detected in the Sn matrix, and the depth was approximately 10 μm.

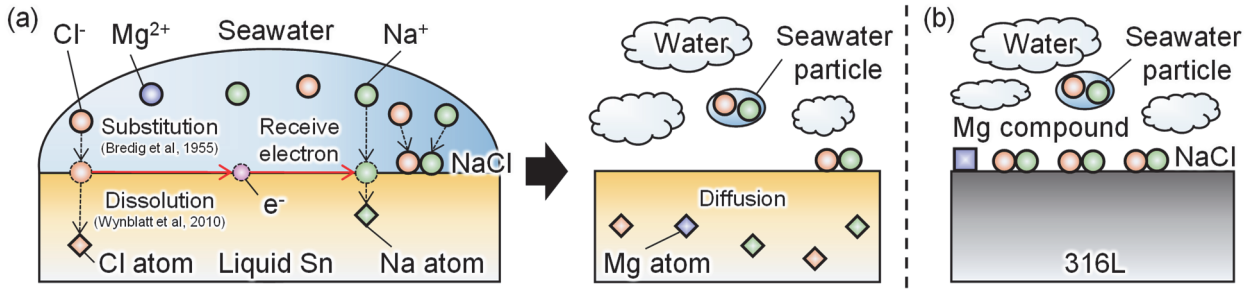

Figure 7. Possible mechanism of mass transfer between artificial seawater droplet and liquid Sn: (a) Dissolution of mineral elements and production of water vapor into liquid Sn and (b) 316L surface.

4. Discussions

Figure 7 shows the schematic diagram of the mass transfer between the droplet of artificial seawater and liquid Sn. The droplet was heated on the surface of liquid Sn, and water vapor was then produced as shown in Figures 7 (a) and (b). The particles of artificial seawater could be produced in this process and they were transferred with the flow of water vapor. Therefore, mineral elements were slightly detected in the distilled water as shown in Figure 3.

The precipitation of NaCl was slightly recognized on the surface of Sn used in the direct contact tests at 573 K and 623 K as shown in Figures 4 (e) and (f). However, Na and Cl were dissolved into liquid Sn according to the results of SEM/EDX analysis. The substitution of Cl^- ions for free electrons [24] might be induced on the liquid Sn surface as shown in Figure 7 (a). Cl^- ions might be dissolved in liquid Sn as a $SnCl_2$ cluster and a non-metal impurity [25,26]. Na^+ ions could then receive free electrons on the surface of liquid Sn and form Na atoms. Na atoms could be dissolved into liquid Sn [27], though the current results could not provide any evidence to support the mechanism that Na and Cl were dissolved in Sn in a metallic state. The Na-Sn phase diagram indicates that the solubility of Na atom in liquid Sn at 573 K is approximately 20 atomic % [27]. The Cl-Sn phase diagram indicates that the solubility of Cl atom in liquid Sn at 573 K is approximately 20 atomic % [26]. The surface of liquid Sn was locally cooled by evaporation of water in the distillation process, and this could make the temperature distribution in liquid Sn. The temperature distribution induced natural convection of liquid Sn, and the convection promoted the mass transfer of the mineral elements in liquid Sn. The formation of Na and Cl enriched region in liquid Sn was mitigated at higher temperature as indicated in Figures 6 (b) and (c). The natural convection could be promoted at higher temperature, since the viscosity of liquid Sn was smaller at higher temperature. The elements dissolved on the Sn surface were then diluted by the mass transfer promoted by the natural convection. The concentration of atomic Cl in the enriched region was smaller than that of atomic Na possibly due to the desorption of Cl in the cooling procedure. These behaviors were different from the surface deposition of salts on the 316L plate which is shown in Figure 7 (b).

5. Conclusion

The distillation of artificial seawater was carried out by direct contact between artificial seawater droplets and liquid metal Sn. The results of ICP-OES analysis on the distilled water indicated that its purity was sufficiently high. The mass transfer of mineral elements such as Na and Cl between artificial seawater and liquid Sn was studied by means of metallurgical analysis on the liquid Sn media used in the direct contact tests. The mineral elements contained in artificial seawater dissolved into liquid Sn. The region enriched with Na and Cl was detected near the surface of Sn matrix. Thermal convection was induced by the temperature distribution made inside liquid Sn since the surface was locally cooled by the evaporation of water. The mass transfer of dissolved elements in liquid Sn was promoted by the thermal convection.

Acknowledgements

Authors would acknowledge Mr. Toshihiko Hara of Institute of Science Tokyo for his technical support on the preparation of the specimens and the experimental apparatus. Authors would acknowledge the staffs of Materials Analysis Division, Core Facility Center of Institute of Science Tokyo for their technical support on the analysis. This paper is partially based on results obtained from a project, JPNP20004, subsidized by the New Energy and Industrial Technology Development Organization (NEDO).

References

[1] M.M. Mekonnen and Y.H. Arjen, Four billion people facing severe water scarcity, *Science Advances* 2 (2016), e1500323.

[2] M.A. Shannon, W.B. Paul, E. Menachem, G.G. John, J.M. Benito and M.M. Anne, Science and technology for water purification in the coming decades, *Nature* 452 (2008), pp. 301-310.

[3] A. Panagopoulos and H. Katherine-Joanne, Environmental impacts of desalination and brine treatment - Challenges and mitigation measures, *Marine Pollution Bulletin* 161 (2020), 111773.

[4] M. Elimelech and A.P. William, The future of seawater desalination: Energy, Technology, and the Environment, *Science* 333 (2011), pp. 712-717.

[5] K.E. Thomas, Overview of village scale, renewable energy powered desalination, (1997), Golden,

Colorado, National Renewable Energy Laboratory.
[6] H. Shemer and S. Raphael, Sustainable RO desalination – Energy demand and environmental impact, *Desalination* 424 (2017), pp. 10-16.
[7] I. Ihsanullah, A.A. Muataz, S. Muhammad and K.N. Mazen, Desalination and environment: A critical analysis of impacts, mitigation strategies, and greener desalination technologies, *Science of The Total Environment* 780 (2021), 146585.
[8] N. Belkin, R, Eyal, E. Hila, K. Nurit and B-F. Ilana, The effect of coagulants and antiscalants discharged with seawater desalination brines on coastal microbial communities: A laboratory and in situ study from the southeastern Mediterranean, *Water Research* 110 (2017), pp. 321-331.
[9] V.G. Gude, Desalination and sustainability – An appraisal and current perspective, *Water Research* 89 (2016), pp. 87-106.
[10] S.H. Ali, G. Damien, A. Nicholas, N. Edmund, B. Graham, D. Alecos, D. Ray, A.E. Maria, K. Judith, L. Anna, D.M. Lawrence, O. Roland, S. Janet, S. Richard, S. Gabi, V. Olivier and Y. Natalia, Mineral supply for sustainable development requires resource governance, *Nature* 543 (2017), pp. 367-372.
[11] M.S. Diallo, R.K. Madhusudhana and C. Manki, Mining critical metals and elements from seawater: opportunities and challenges." *Environmental Science & Technology* 49 (2015), pp. 9390-9399.
[12] M. Takahashi, S. Uchida and Y. Kasahara, Design study on reactor structure of Pb-Bi-cooled direct contact boiling water fast reactor (PBWFR), *Progress in Nuclear Energy* 50 (2008), pp. 197-205.
[13] H. Branover, E-B. Arik, G. Ehud and B. Amitzur, Promising applications of the liquid metal MHD energy conversion technology, in William D. Jackson and Dorothy A. Hull (Eds.), *Proceedings of the 24th Intersociety Energy Conversion Engineering Conference* 2, (1989), pp. 1051-1058, New York, IEEE.
[14] P.N. Martynov and D.I. Konstantin, Properties of lead-bismuth coolant and perspectives of non-electric applications of lead-bismuth reactor, in Toshio Konishi and Georg Woite (Eds.), *IAEA-TECDOC-1056* (1997), pp. 177-184, Vienna, IAEA.
[15] P.N. Martynov, V.D. Andrey, I.O. Yu and A.G. Valery, Water and hydrogen in heavy liquid metal coolant technology, *Progress in Nuclear Energy* 47 (2005), pp. 604-615.
[16] M. Kondo and Y. Nakajima, Boiling points of liquid breeders for fusion blankets, *Fusion Engineering and Design* 88 (2013), pp. 2556-2559.
[17] M. Kondo, T. Tanaka, S. Fukada and V. Tsisar, 6.06 Liquid Breeder Materials, in Rudy J. M. Konings and Roger E. Stoller (Eds.) *Comprehensive Nuclear Materials (Second Edition)*, (2020) pp. 176-202, Oxford, Elsevier Science.
[18] S.A. Alizadeh Tabatabai, Coagulation and ultrafiltration in seawater reverse osmosis pretreatment, Leiden, the Netherlands, CRC Press/Balkema.
[19] M. Kondo, Y. Hishinuma, T. Norimatsu and T. Muroga, Corrosion-erosion and mass transfer dynamic behaviors of reduced activation ferritic/martensitic steel in a nonisothermal Pb-17Li system, *Fusion Engineering and Design* 136 (2018), pp. 1581-1587.
[20] M. Kondo, Y. Nakajima, T. Tanaka, T. Nozawa and T. Yokomine, Experimental study on chemical behaviors of non-metal impurities in Pb, Pb-Bi and Pb-Li by temperature programmed desorption mass spectrometer analysis, *Plasma and Fusion Research* 11 (2016), 2405076.
[21] H. Asegun and R. Prasher, The prospect of high temperature solid state energy conversion to reduce the cost of concentrated solar power, *Energy & Environmental Science* 7 (2014), pp. 1819-1828.
[22] World Health Organization, *Guidelines for drinking-water quality*, 4th edition, incorporating the 1st addendum, Geneva, World Health Organization.
[23] M. Hori, K. Shozugawa, K. Sugimori and Y. Watanabe, A survey of monitoring tap water hardness in Japan and its distribution patterns, *Scientific Reports* 11 (suppl.2) (2021), pp. S3-4.
[24] M.A. Bredig, J.W. Johnson, and Wm T. Smith Jr., Miscibility of Liquid Metals with Salts. I. The Sodium-Sodium Halide Systems, *Journal of the American Chemical Society* 77 (1955), pp. 307-312.
[25] P. Wynblatt, S. Curiotto and D, Chatain, A model of oxygen adsorption at liquid copper surfaces, *Surface Science* 604 (2010), pp. 1369-1376.
[26] H. Okamoto, Cl-Sn (Chlorine-Tin), *Journal of Phase Equilibria and Diffusion* 34 (2013), p. 1136.
[27] A.J. Sangster, J. Alan and W.B. Christoper, The Na-Sn (Sodium-Tin) system, *Journal of Phase Equilibria* 19 (1998), pp. 76-81.